BRITTLE FRACTURE IN CHARPY IMPACT TEST

INFLUENCE OF MATERIAL PARAMETERS

JULES ROYER

March 22, 2024

CONTENTS

1 INTRODUCTION

Goal of this work is to analyze the conditions under which fractures and cracks propagate in materials. It relies on the theory of fracture mechanics. It has many important applications, especially in the industry field, in which built mechanical components often have flaws. The probability of the failure of the material during its operation must be assessed. To that end, engineers do a damage tolerance analysis. The Charpy impact test is commonly used to study fractures. Its functioning is quite simple: a striker is dropped and hits a notched tensile, the difference between the final and initial heights correspond to the energy dissipated in the specimen to create a fracture.

In this work, Finite Element Element simulations of this experiment are done to analyze the influence of some parameters of the material on its resistance to fracture.

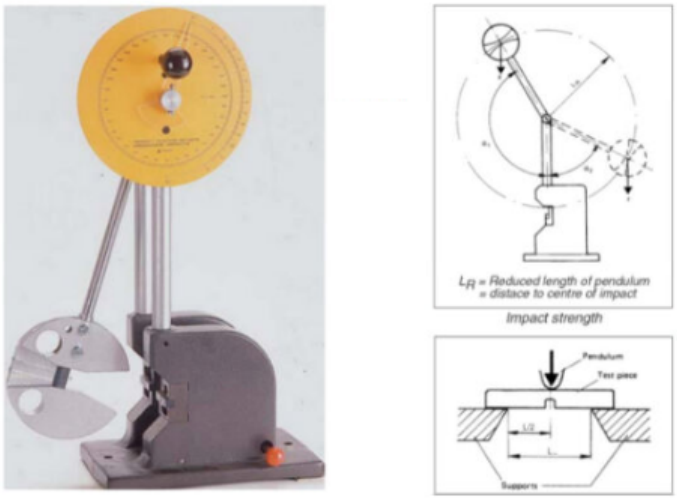

Figure 1: Charpy impact machine picture and a sketch explaining how it works.

2 PRELIMINARY FINITE ELEMENT MODEL

We present here a FEM model of the Charpy specimen. Here it is a tensile with dimensions $L = 55\text{mm}, W = 10\text{mm}, H = 10\text{mm}$. It has an isotropic elastic behavior under low strain or stress, with a Young Modulus $E = 208\text{GPa}$ which is standard for steel. It then has a isotropic non linear plastic behavior ruled by the following yield function: $f(\sigma, p) = \sigma_{eq} - R_0 - Q(1 - \exp^{-bp})$ where p is the cumulative plastic deformation $p = \int_{t=0}^{t=t*} \varepsilon_p(t)dt$, and the fitted parameters are $R_0 = 510\text{MPa}, Q = 314.62\text{MPa}, b = 16.13$.

To model the plastic regime, the *Von Mises* equivalent stress is used:

$$\sigma_{eq} = \sqrt{\frac{1}{2}\left((\sigma_1 - \sigma_2)^2 + (\sigma_2 - \sigma_3)^2 + (\sigma_3 - \sigma_1)^2\right)} \tag{1}$$

Where σ_i are the principal stresses. Lastly, the Beremin model is used to predict the evolution of the crack. Concerning the boundary conditions, anvils on which the specimen lies are immobile, the striker has a prescribed vertical downward movement, also called loas, at constant speed $\dot{u}_2 = -1\text{mm.s}^{-1}$. The ligament, ie the nodes of the FEM mesh in the vertical plane cutting the specimen in half, are also immobile along the horizontal axis. While this assumption is not physically justified, it is useful to shrink the problem's size to only the right half of all aforementioned objects, because the problem can be considered symmetrical along the ligament.

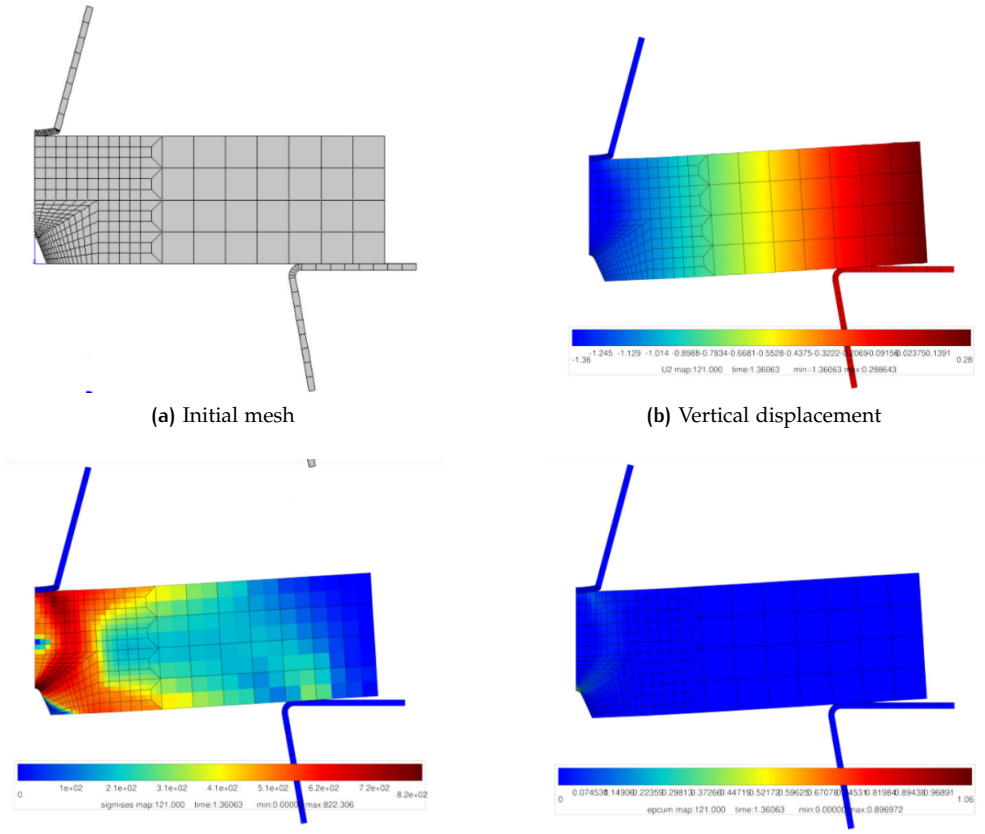

(a) Initial mesh

(b) Vertical displacement

(c) *Von Mises* stress

(d) cumulative plastic deformation

Figure 2: Results of experiment 1

The first simulation returned an error during the last iterations. We observe a concentration of high *Von Mises* stress around the notch and near the striker, $\sigma_{eq} > 700$MPa, and also a bit of plastic deformation. A possible explanation of the error could be a lacking mesh precision around those zones and also near the anvils where it reaches ~ 310MPa.

3 LOCAL MESH REFINEMENT

Thanks to this analysis, we choose a finer mesh in those areas :

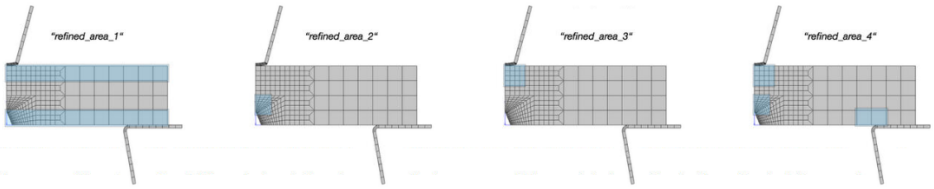

Figure 3: Propositions of mesh refinement.

The 4-th mesh fulfills our desires of refinement, so we select it. In order to select the size of the smallest mesh elements, we rerun the previous experiment with $40\mu m, 10\mu m, 4\mu m$:

With these finer meshes, the previous simulation now converges. Results on Figures 4b and 4c quite differ between $40\mu m$ and the 2 smaller sizes, meaning

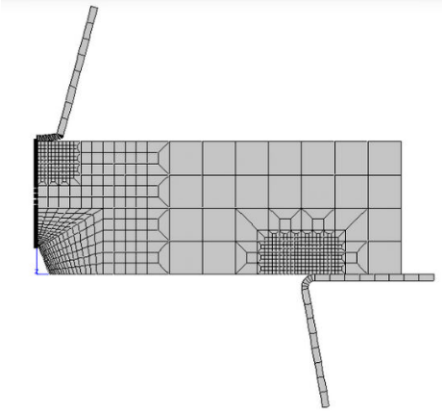

(a) Refined mesh

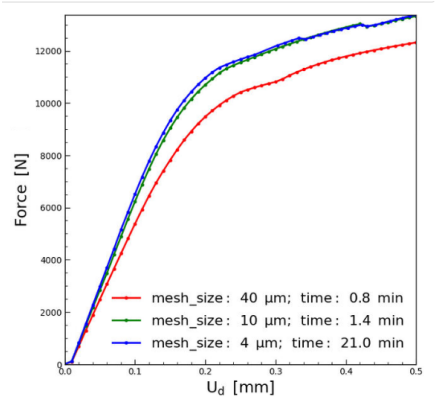

(b) Relation force on striker - displacement

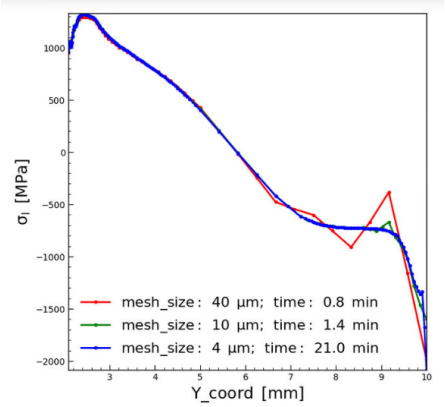

(c) Relation first principal stress - y coordinate

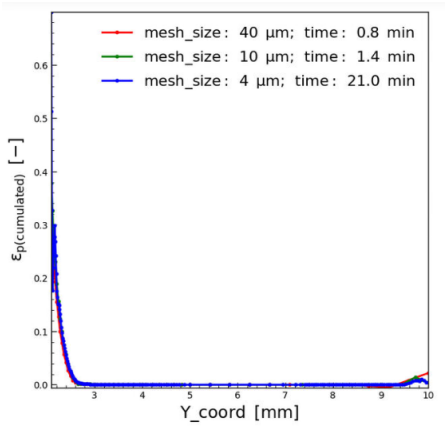

(d) Relation cumulative plastic deformation - y coordinate

Figure 4: Comparison of mesh refinements.

some model accuracy is gained with refinement. However, 10µm and 4µm have similar results for the desired precision, but the 10µm simulation was 15 times faster, therefore it is more interesting for us to choose it instead of the smallest size. We see again on Figures 4c and 4d the concentration of stress and plastic deformation near the notch ie in the low y zones.

4 GEOMETRIC PARAMETER SENSITIVITY

Now that a more adapted mesh is found and simulations converge, it is interesting to assess the dependency of the geometry of the Charpy specimen in its probability of failure. Numerical simulation is here useful to run multiple Charpy tests, that in reality are hard to set up. The considered parameters are the notch radius N_R, the height H and half of the width H_W:

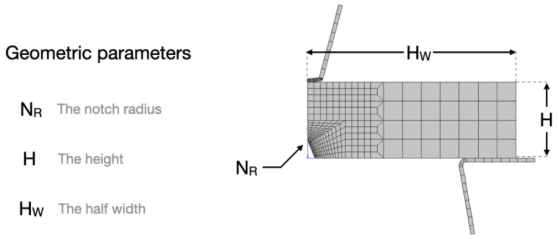

Figure 5: Considered geometric parameters.

The strategy is here to run 3 simulations for each parameter, in each of them we add a certain variation of the parameter: −20%, 0% and +20%, while keeping every other at its default value.

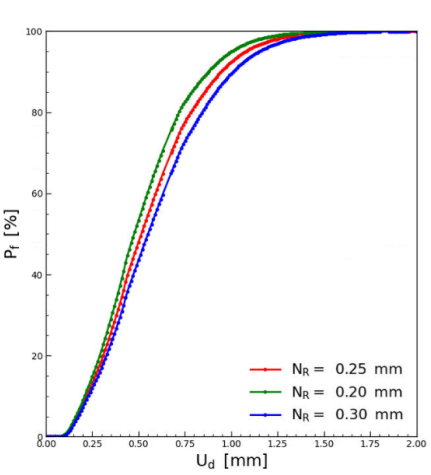

(a) Probability of failure for various N_R

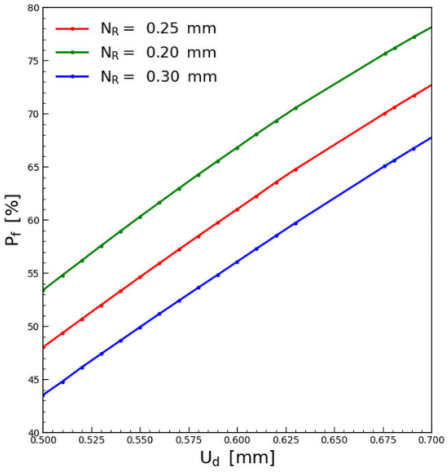

(b) Zoom

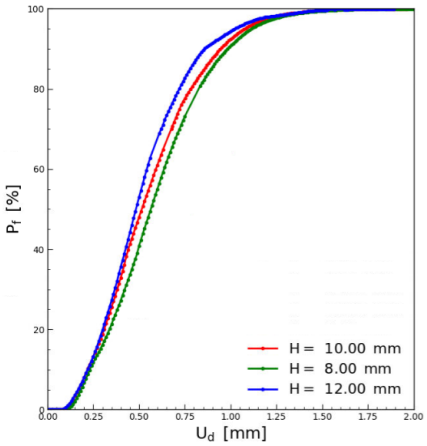

(c) Probability of failure for various H

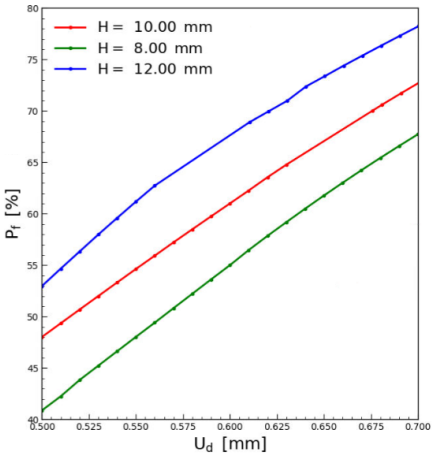

(d) Zoom

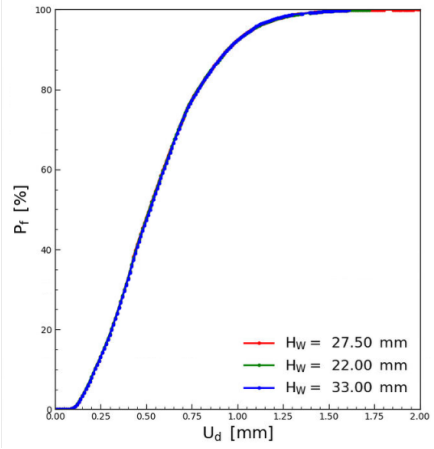

(e) Probability of failure for various H_W

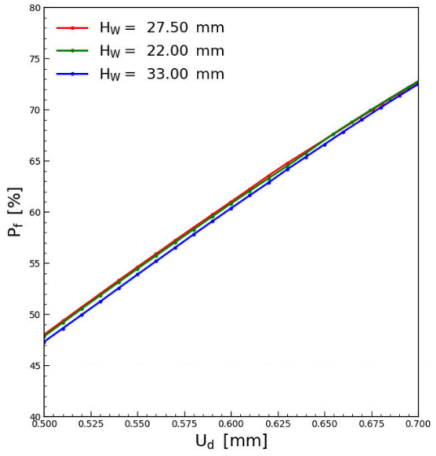

(f) Zoom

Figure 6: Probability of failure with respect to the striker displacement for various values of N_r, H and H_W.

On Figure 6, we see that the probability of failure curve has a similar shape for each parameter. The plots of the right column are zooms on the zones of highest variance between curves, with $U_d \in [0.5\text{mm}, 0.7\text{mm}]$. On these zooms, all P_f curves are approximately linear, with same slope $\frac{\Delta P_f}{\Delta U_d} \sim \frac{72-48}{0.7-0.5} = 120\%.\text{mm}^{-1}$. Only the offsets at a given displacement u_d differ between parameters variations

$\nu_1, \nu_2 \in \{\pm 20\%, 0\%\}$ ie $|P_{f,\nu_1}(u_d) - P_{f,\nu_2}(u_d)|$. Variating H_W by $\pm 20\%$ induces the smallest variation of P_f, of $\sim 1\%$, where for N_R and H, $\Delta P_f \sim 5\%$. Therefore H and N_R are the 2 most impactful parameters on the failure probability. The lower the notch radius and the higher the height, the higher the failure probability. Such a result can be misleading at first sight, but recall that N_R is measured at a fixed height, and therefore a smaller N_R is linked to a sharper angle at the origin of the notch. Consequently, sharp geometries tend to concentrate the stress on them and therefore increase the probability of failure. For H, a possible interpretation is the increase of the population of defects with the height. But if one industrial operator should choose to focus only on one parameter, H seems simpler to adjust than N_R, eventhough the latter seem more dangerous, because the failure probability increases as N_R diminishes, which makes the notch harder to spot.

5 THE BEREMIN MODEL

A difficulty linked to estimating the failure probability is that failure sometimes appear eventhough the applied stress is below the yield value of the material, because there were defects and cracks in it at a microscopic scale. The Beremin model focuses on linking a macroscopic fracture to those micromechanisms.

The idea of the Beremin model relies on 2 main assumptions. The first states that microcracks appear due to a plastic deformation in grains, that is inhomogeneous because of initial defects. The second models the propagation of those microcracks with a probabilistic failure parameter, σ_w exceeding a critical value. To infer a macroscopic fracture from the microscopic state, Beremin's model relies on the weakest link theory stating that the latter occurs when a microcracks is submitted to the Griffith stress σ_c. Equivalently, the fracture occurs when a microcrack reaches a length of $l_{0c} = 2E\gamma_s/(\delta\sigma_c^2)$ where $\delta \sim 1$ is constant and γ_s is the effective surface energy. As mathematical tools, Beremin relies on a generalized extremum law of probability called the Weibull distribution. For the initial distribution $\mathbb{P}_{crack}$ of defects, a power law is commonly used, leading to the probability of failure of an element of volume V_0 under a stress σ:

$$\mathbb{P}_{V_0,fail}(\sigma) = \int_{l_{0c}}^{+\infty} \mathbb{P}_{crack}(l_0)dl_0 = \int_{l_{0c}}^{+\infty} \frac{\alpha}{l_0^\beta} dl_0 \tag{2}$$

Where α, β are material constraints. By only considering plane strain condition, the probability of failure is calculated with:

$$P_f = 1 - \exp\left(-\frac{\frac{1}{V_0}\int_{V_p} \sigma_I^m dV}{\sigma_u^m}\right) = 1 - \exp\left(-\left(\frac{\sigma_w}{\sigma_u}\right)^m\right) \tag{3}$$

Where $m = 2\beta - 1$ is the Weibull shape factor, $\sigma_w = \left(\frac{1}{V_0}\int_{V_p} \sigma_{I,p}^m\right)^{\frac{1}{m}}$ is the Weibull stress, V_p the plastic volume, $\sigma_I(V)$ the principal stress on the local volume V and $\sigma_u = (m/2\alpha)^{\frac{1}{m}}\sqrt{2E\gamma_s\delta}$ is the Weibull scale factor.

The 2 Beremin parameters m and σ_u have specific influence on P_f: m is linked to the distribution of length of microcracks (Eq 2). Its increase favors smaller lengths of defects (with $\alpha^{\frac{1}{m}}$ as reference of length). To assess its impact on P_f, we can assume σ_w is approximately constant when m varies, then an increase of m increases P_f if $\sigma_w > \sigma_u$ and decreases it if $\sigma_w < \sigma_u$. For σ_u, its increase induces a decrease of P_f, it is a kind of a macroscopic stress threshold under which the material can resist.

Looking at the results of simulations on the Figure below, the trend that m shifts the curve of P_f to the right is visible, without noticeably changing the slope, prob-

ably because the variation of σ_w w.r.t m must be considered. As expected, a σ_u reduces the slope in the linear part.

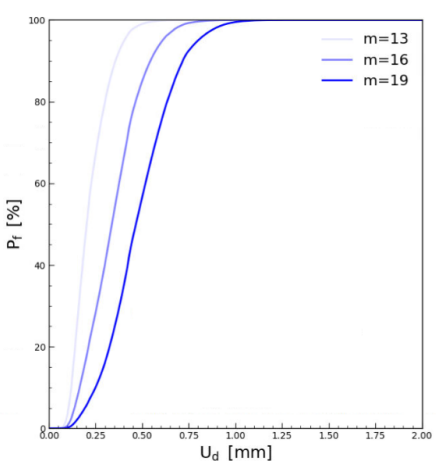

(a) Probability of failure for various m.

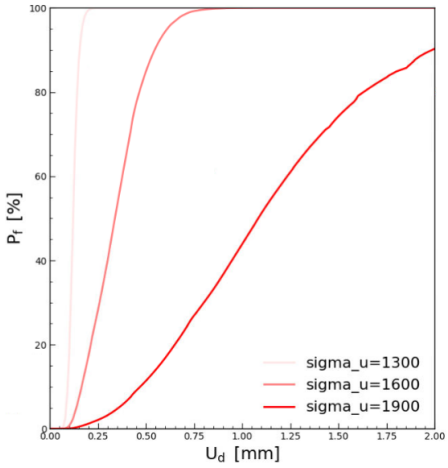

(b) Probability of failure for various σ_u.

We wish now to find m and σ_u for a given material, for which we experimentally statistics of failure P_f for load u_d. Because the FEM model has long computation time, a regression approach will be very time consuming. In fact, one simulation that computes u_d, P_f given m, σ_u takes ~ 1 minute. Therefore it is preferable to adjust manually those parametres, knowing their influence as explained before. Pretty quickly a satisfying estimation has been found on Figure 7.

The mean square error of the estimation interpolated on the experimental values of u_d is $\sum_{u_{d,exp}} \left(P_{f,exp}(u) - P_{f,sim}(u)\right)^2 = 10.14$. An optimisation algorithm that minimized the mean square error gave as solutions $m_{opt} = 16$ and $\sigma_{u,opt} = 1800$ and an error $e_{opt} \sim 4$, so quite lower as the previous estimation.

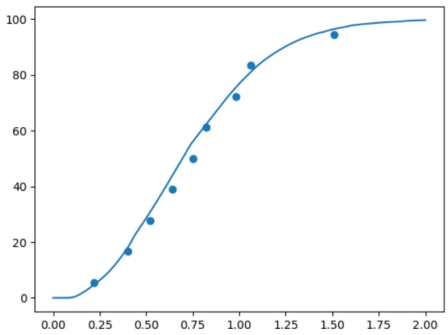

Figure 7: Observed $P_f(u_d)$ (blue dots). Estimated $P_f(u_d)$ with FEM method (blue curve) and $m = 15, \sigma_u = 1830$.

6 EFFECT OF THE TEMPERATURE

An interesting question that occurs frequently in manufacturing is the influence of the temperature on the failure probability. Multiples simulation have been conducted to estimate the variation of σ_w and P_f with different temperatures. Results are in Figure 8.

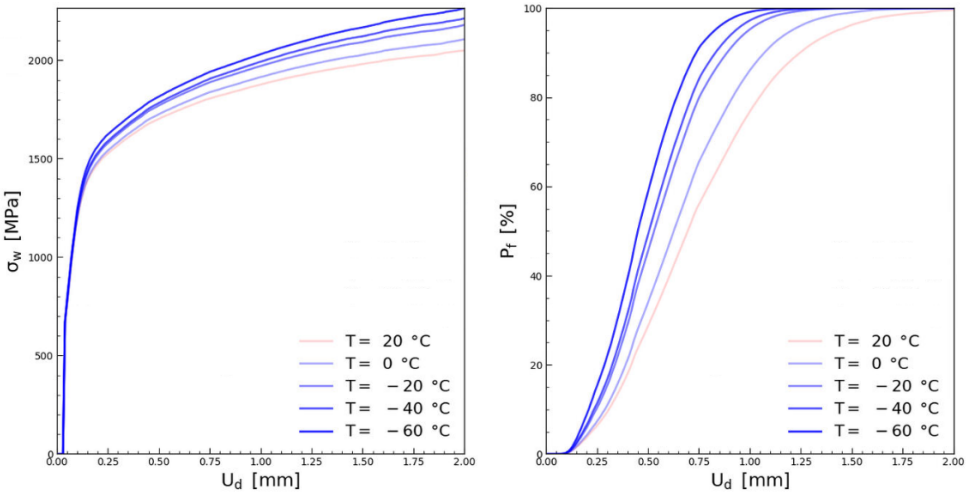

Figure 8: Variations of σ_w and P_f with different temperatures

The curves of $u_d \to \sigma_w(u_d)$ have same linear slope near the origin, and different asymptotic straight lines. As T decreases, the offset and the slope of those lines increases, meaning that it increases the local stress on the plastic volume. A possible interpretation is that lowering T slow down the particles' movements and therefore hinders the material's deformation in response to the applied stress, as it makes the material more brittle. Similarly, lowering T shift the curve of P_f to the left and increases the slope, meaning it increases the chances of failure for all load displacements u_d.

7 CONCLUSION

In this work, a Finite Element Model of the Charpy impact test has been used in order to assess the influence of various parameters on the resistance of a notch material, ie its ability not to fracture when it is subject to a stress near the notch. Firstly the mesh near the highly stressed zones had te be refined in order to have convergent simulations, and then a sensitivity analysis of 3 geometrical parameters: N_R the notch radius, H the height of the specimen and H_W half of its width, on the probability of failure P_f has been conducted : . As a result, both N_R and H had a significant influence on the failure probability, and therefore should be watched in an industrial context. The study has then assessed the effect of the 2 main parameters of the Beremin Model, a local probabilitic approach to fracture model that links the fracture of the material to the lengths of its microcracks. CCL Beremin.

Lastly the increase of P_f with a lowering of the temperature has been observed on simulations and the induced hindering on the movements of particles has been given as an interpretation.

As a sequel of this work, a study on the influence on the resistance of context-specific environmental properties to which the material is exposed can be interesting, especially on the irridiation levels, that typically occur in nuclear infrastructures. Multiple studies focus on this issue and link it to the material's composition. As an example, levels of copper, nickel and phosphorus matter when one studies the irradiation effects.

One limitation of the Beremin Model used here is its inability to model inhomogeneities in the material. To that end, an extended version, called the bi-modal Weibull distribution has been developped.